Research Article

Investigating the Sterile Neutrino Parameters with QLC in 3 + 1 Scenario

Gazal Sharma [iD] and B. C. Chauhan [iD]

Department of Physics and Astronomical Science, School of Physical and Material Sciences,
Central University of Himachal Pradesh (CUHP), Dharamshala, Kangra, Himachal Pradesh 176215, India

Correspondence should be addressed to Gazal Sharma; gazzal.sharma555@gmail.com

In the scenario with four generation quarks and leptons and using a 3 + 1 neutrino model having one sterile and the three standard active neutrinos with a 4×4 unitary transformation matrix, U_{PMNS_4}, we perform a model-based analysis using the latest global data and determine bounds on the sterile neutrino parameters i.e., the neutrino mixing angles. Motivated by our previous results, where, in a quark-lepton complementarity (QLC) model we predicted the values of $\theta_{13}^{PMNS} = \left(9_{-2}^{+2}\right)^{\circ}$ and $\theta_{23}^{PMNS} = \left(40.60_{-0.3}^{+0.1}\right)^{\circ}$. In the QLC model the nontrivial correlation between CKM_4 and $PMNS_4$ mixing matrix is given by the correlation matrix V_{c_4}. Monte Carlo simulations are performed to estimate the texture of V_{c_4} followed by the calculation of $PMNS_4$ using the equation, $U_{PMNS_4} = \left(U_{CKM_4} \cdot \psi_4\right)^{-1} \cdot V_{c_4}$, where ψ_4 is a diagonal phase matrix. The sterile neutrino mixing angles, θ_{14}^{PMNS}, θ_{24}^{PMNS} and θ_{34}^{PMNS} are assumed to be freely varying between $(0 - \pi/4)$ and obtained results which are consistent with the data available from various experiments, like NoνA, MINOS, SuperK, Ice Cube-DeepCore. In further investigation, we analytically obtain approximately similar ranges for various neutrino mixing parameters $\left|U_{\mu 4}\right|^2$ and $\left|U_{\tau 4}\right|^2$.

1. Introduction

After the completion of a few decades since the birth of Neutrino Physics and its experimental world, we are at a stage where we have unraveled various mysteries, including very strong evidence of neutrinos being massive and the existence of neutrino oscillation, but there are many issues that still need to be resolved. The recent results from Daya Bay, CHOOZ, and other experiments [1–5] on the relatively large value of θ_{13}^{PMNS}, a clear 1st-order picture of the three flavor lepton mixing matrix have emerged [6–8]. So, according to the current experimental situation we have measured all the quark and charged lepton masses, and the value of the difference between the squares of the neutrino masses $\Delta m_{12}^2 = m_2^2 - m_1^2$ and $\left|\Delta m_{23}^2\right| = \left|m_3^2 - m_2^2\right|$. We also know the value of the quark mixing angles and the mixing angles, θ_{12}^{PMNS}, θ_{23}^{PMNS}, and θ_{13}^{PMNS} in the lepton sector. The way the Cabibbo-Kobayashi-Maskawa $\left(U_{CKM}\right)$ mixing matrix is there in quark sector, the phenomenon of lepton flavor mixing is described by a 3×3 unitary

matrix called Pontecorvo-Maki-Nakagawa-Sakata $\left(U_{PMNS}\right)$. Investigating global data fits of the experimental results, so far we have got a picture which suggests that the U_{PMNS} matrix contains two large and a small mixing angles; i.e., the $\theta_{23}^{PMNS} \approx 45^{\circ}$, the $\theta_{12}^{PMNS} \approx 34^{\circ}$ and the $\theta_{13}^{PMNS} \approx 9^{\circ}$.

These results when read along with the quark flavor mixing matrix $\left(U_{CKM}\right)$, which is quite settled with three mixing angles that are small i.e., $\theta_{12}^{CKM} \approx 13^{\circ}$, $\theta_{23}^{CKM} \approx 2.4^{\circ}$ and $\theta_{13}^{CKM} \approx 0.2^{\circ}$, a disparity-cum-complementarity between quark and lepton mixing angles is noticed. Since the quarks and leptons are fundamental constituents of matter and also those of the Standard Model(SM), the complementarity between the two of them is seen as a consequence of some symmetry at high energy scale. This complementarity popularly named "Quark–Lepton Complementarity" (QLC) has been explored by several authors [9–14]. The relation is quite appealing to do the theory and phenomenology; however, it is still an open question, what kind of symmetry could be there between these fundamental particles of two sectors. The possible consequences of the QLC

have been widely investigated in the literature. In particular, a simple correspondence between the U_{PMNS} and U_{CKM} matrices have been proposed and used by several authors [15–18] and analysed in terms of a correlation matrix V_c [19–22].

The fact that lepton flavors mix as well as oscillate leads to a new window of physics beyond the SM. Neutrino mixing may fill many voids of SM but still, there are few anomalies that could not be explained within the three flavor framework of neutrinos and points towards the existence of another flavor of neutrinos i.e., (*sterile neutrino*) with a mass ~ eV scale. Sterile neutrinos are the singlets of the Standard Model gauge symmetries that can couple to the active neutrinos via mixing only. Till now there are bounds on the active-sterile mixing, but there is no bound on the number of sterile neutrinos and on their mass scales. The existence of sterile neutrinos is investigated at different mass scales by various experiments; LSND, MiniBooNE, MINOS, Daya Bay, IceCube, etc.

The main motivation behind this work is basically testing our model in the 4th generation scenario. After the successful results obtained in our previous papers, we have tried to extend our model and complete analysis in 3 + 1 scenario. Along with that the major motivating factor that pushed us towards the extension of our model in 3 + 1 scenario is that the results obtained in our previous works [19–22] (*and references therein*) are quite consistent with the recent results from NoⅴA [23] and IceCube [24] which give us new ray of hope in favour of our model and its stability. Taking into account the precise results obtained from various experiments on neutrino mixing angles for three generations our model and its predictions fit quite well. As we all are aware of the fact that with the pace of time we are entering into the better precision era, considering that we have tried to extend our analysis to 3 + 1 scenario with more accurate Wolfenstein parameters for U_{CKM_4} and neutrino mixing parameters for U_{PMNS_4} preserving unitarity up to 4th order. Using all the parameters that are available from the global data analysis we tried to investigate the structure of the 4 × 4 correlation matrix V_{c_4}, numerically. According to our investigations, there is a possibility of the existence and role of sterile neutrinos in the QLC, that helped us to give some constrained results for two sterile neutrino mixing angles i.e., θ_{24}^{PMNS} and θ_{34}.

On the stability of the framework that we have used in order to carry out our entire analysis which is the extension of SM in 4th generation, one might argue that the four generation scenarios are strongly disfavoured. This is true, unless a substantial modification is realized for the scalar sector. However, such an extension of the Standard Model (with massive neutrinos) is excluded by several authors eg., in [25, 26]. As such, during the starting period of the discovery of Higgs particle, data were not so precise that the possibility of the 4th generation coupling to the Standard Model Higgs doublet was not introduced in a different Beyond Standard Model scenarios. But, such options were ruled out as the LHC data develops gradually, which let many scenarios to go beyond SM(BSM). It has been noted that such 4th generation is hidden during the single production of the Higgs Boson, while it shows up when one considers the double Higgs production i.e., $gg \rightarrow hh$ which can be considered in a different framework of a two Higgs doublet model (2HDM) [27–30]. This is the framework

that we have taken to carry out our analysis which is well favoured by the work done and published in 2018 [31]. In that work, they show that the current Higgs data do not eliminate the possibility of a sequential 4th generation that gets their masses through the same Higgs mechanism as the first three generations.

In this paper, we have compared our data with the recent results provided by some ongoing experiments. Starting from the beginning of the sterile neutrino search by LSND and MiniBooNE anomalies we have covered a long distance till these recent experiments like NoⅴA, SuperK, MINOS, and Ice Cube-DeepCore and many more for the search of sterile neutrinos. In this paper, we do not comment upon or explain the generation of sterile neutrinos or the 4th generation quarks instead we have used the QLC model and done some numerical analysis to obtain bounds on the values of sterile neutrino parameters using previously formulated U_{PMNS_4} and U_{CKM_4} [32–35].

The paper is organized into five sections as follows. In the next Section 2, we describe in brief the theory of the QLC model and show how this model fits in the 3 + 1 scenario. For the generation of 4 × 4 V_{c_4} matrix, different parametrizations were taken for formulation of U_{CKM4} and U_{PMNS4} and all that is discussed in Section 2. The investigation of correlation matrix (V_{c_4}), using Monte Carlo simulation is done in Section 3. The PMNS matrix followed by the constrained values of sterile neutrino angles is obtained using the model equation in Section 4 along with the results obtained using the QLC model are compared with bounds given by the global data analysis and various experiments. Finally, the conclusions are summarized in Section 5. Various plots(contour and scattered plots) have been made in order to show the correlation between the θ_{24} & θ_{34} and $|U_{\mu4}|^2$ & $|U_{\tau4}|^2$ as well as for $\sin^2\theta_{24}$ and $\sin^2\theta_{34}$ against $\sin^2\theta_{12}$ and $\sin^2\theta_{23}$. We have also obtained the normal distribution function histograms for both θ_{24} and θ_{34} for different values of $m_{t'} = 400/600 GeV$.

2. Theoretical Framework of QLC Model in 3+1 Scenario

The mixing of quarks and leptons has always been of great interest and remains a mystery in particle physics. The search for symmetry or unification of quarks and leptons is one of the goals of particle physics, and many efforts are devoted toward this work. The bottom-up approach i.e., finding some phenomenological relations as well as their explanations, gives some clues on this issue. In the SM the mixing of quark and lepton sectors is described by the matrices U_{CKM} and U_{PMNS}. When we observe a pattern of mixing angles of quarks and leptons, and combine them with the pursuit for unification i.e., symmetry at some high energy leads the concept of quark-lepton complementarity i.e., QLC. Possible consequences of QLC have been widely investigated in the literature and in particular, a simple correspondence between the PMNS and CKM matrices have been proposed and analysed in terms of a correlation matrix V_c. As long as quarks and leptons are inserted in the same representation of the underlying gauge group at some higher energy scale, we need to include in our

definition of V_c arbitrary but nontrivial phases between the quark and lepton matrices. Hence, we will generalise the relation

$$V_c = U_{CKM} \cdot U_{PMNS} \text{ to } V_c = U_{CKM} \cdot \psi \cdot U_{PMNS}, \quad (1)$$

where V_c is the correlation matrix defined as a product of U_{PMNS} and U_{CKM}.

When sterile neutrinos are introduced in the $3 + N_s$ schemes, where the $N_s(N_s = 1$ for one sterile mixing) is the number of new mass eigenstates. For this case, we define ψ_4 in place of ψ in equation (1). So, along with ψ_4 in QLC the above equation takes the form

$$V_{c_4} = U_{CKM_4} \cdot \psi_4 \cdot U_{PMNS_4}, \quad (2)$$

where the quantity ψ_4 is a diagonal matrix $\psi_4 = diag(e^{\iota \psi_i})$ and the four phases of ψ_i are set as free parameters because they are not restricted by present experimental evidences. The $3 + 1$ active-sterile mixing scheme is a perturbation of the standard three-neutrino mixing in which the 3×3 unitary mixing matrix U is extended to a 4×4 unitary mixing matrix with $|U_{e4}|, |U_{\mu 4}|$, and $|U_{\tau 4}|$ which leads to the generation of U_{PMNS_4} lepton mixing matrix. However, the addition of a 4th generation to the standard model leads to a 4×4 quark mixing matrix U_{CKM_4}, which is an extension of the Cabibbo-Kobayashi-Maskawa (CKM) quark mixing matrix in the standard model.

2.1. CKM_4 and $PMNS_4$ Formulation. In order to calculate the texture of V_{c_4} we have used the U_{CKM_4} and U_{PMNS_4} taking reference from several works. Although the 4th generation quarks are too heavy to produce in LHC, yet they may affect the low energy measurements, such as the quark t' would contribute to $b \to s$ and $b \to d$ transitions, while the quark b' would contribute similarly to $c \to u$ and $t \to c$ [32–34].

The CKM matrix in SM is a 3×3 unitary matrix while in the SM_4 (this is the simplest extension of the SM, and retains all of its essential features: it obeys all the SM symmetries and does not introduce any new ones), the U_{CKM_4} matrix is 4×4, matrix which can be shown as

$$U_{CKM} = \begin{bmatrix} V_{ud} & V_{us} & V_{ub} \\ V_{cd} & V_{cs} & V_{cb} \\ V_{td} & V_{ts} & V_{tb} \end{bmatrix}, \quad (3)$$

$$U_{CKM_4} = \begin{pmatrix} \widetilde{V}_{ud} & \widetilde{V}_{us} & \widetilde{V}_{ub} & \widetilde{V}_{ub'} \\ \widetilde{V}_{cd} & \widetilde{V}_{cs} & \widetilde{V}_{cb} & \widetilde{V}_{cb'} \\ \widetilde{V}_{td} & \widetilde{V}_{ts} & \widetilde{V}_{tb} & \widetilde{V}_{tb'} \\ \widetilde{V}_{t'd} & \widetilde{V}_{t's} & \widetilde{V}_{t'b} & \widetilde{V}_{t'b'}, \end{pmatrix}, \quad (4)$$

where all the elements of the matrix have their usual meanings except for b' and t', which we have already defined above. In the presence of the sterile neutrino ν_s, the flavor ($\nu_\alpha, \alpha = e, \mu, \tau, s$) and the mass eigenstates ($\nu_i, i = 1, 2, 3, 4$) are connected through a 4×4 unitary mixing matrix U, which depends on six complex parameters [36, 37]. Such a matrix can be expressed as the product of six complex elementary rotations, which define six real mixing angles and six CP-violating phases. Of these phases three are of the Majorana type and are unobservable in oscillation processes, while the remaining three are of the Dirac type.

A particularly convenient choice of the parametrization of the mixing matrix is

$$U = \widetilde{R}_{24} R_{34} \widetilde{R}_{14} R_{23} \widetilde{R}_{13} R_{12} P, \quad (5)$$

where R_{ij} and $\widetilde{R}_{ij}$ represent a real and complex 4×4 rotation in the (i, j) plane, respectively containing the 2×2 sub matrices

$$R_{ij}^{2 \times 2} = \begin{bmatrix} C_{ij} & S_{ij} \\ -S_{ij} & C_{ij} \end{bmatrix}, \quad (6)$$

$$\widetilde{R}_{ij}^{2 \times 2} = \begin{bmatrix} C_{ij} & \widetilde{S}_{ij} \\ -\widetilde{S}_{ij}^* & C_{ij} \end{bmatrix}, \quad (7)$$

where $C_{ij} \equiv \cos \theta_{ij}$, $S_{ij} \equiv \sin \theta_{ij}$ and $\widetilde{S}_{ij} \equiv S_{ij} e^{-\iota \phi_{ij}}$.

3. Numerical Simulation and Methodology

In the standard parametrization of U_{CKM} and U_{PMNS} in equation, we have inserted the observed/experimental values of the U_{CKM} and U_{PMNS} parameters, and obtained the probability density texture of the correlation matrix (V_c) using Monte Carlo method for 1 billion shots for each variable. We have fully used freedom of the unknown parameters like ψ and ϕ by varying them in the unconstrained spread $[0 - 2\pi]$ with flat distribution. Now, we write

$$U_{PMNS_4} = \left(U_{CKM_4} \cdot \psi_4 \right)^{-1} \cdot V_{c_4}, \quad (8)$$

this expression is the inverse of equation (2), which was used to estimate the texture of the correlation matrix V_{c_4}.

Using equation (8) we have reverted the results of the exercise in order to predict the unknown sector of U_{PMNS}. In the inverse equation the generalised correlation matrix V_{c_4} thus obtained was basically used to be replaced by bimaximal (BM) and tribimaximal (TBM) matrices in the previous year by several authors [19–22] (*and references therein*).

As such, this model procedure using numerical method of Monte Carlo and freedom of unknown parameters is having merit as its predictive power shown in our previous works published in quality journals [19–22].

The U_{CKM_4} matrix can be described, with appropriate choices for the quark phases, in terms of 6 real quantities and 3 phases. We have used the Dighe-Kim (DK) parameterization of the CKM_4 matrix [32–34]. This matrix can be calculated in the form of an expansion in powers of λ such that each element is accurate up to a multiplicative factor of $\left[1 + O\left(\lambda^3 \right) \right]$. The Dighe-Kim (DK) parametrization defines

$$\begin{aligned} \widetilde{V}_{ud} &= 1 - \frac{\lambda^2}{2}, \\ \widetilde{V}_{us} &= \lambda, \quad (9) \\ \widetilde{V}_{ub} &= A\lambda^3 C e^{\iota \delta_{ub}}, \end{aligned}$$

$$\begin{aligned} \widetilde{V}_{ub'} &= p\lambda^3 e^{-\iota \delta_{ub'}}, \\ \widetilde{V}_{cd} &= -\lambda, \quad (10) \\ \widetilde{V}_{cs} &= 1 - \frac{\lambda^2}{2}, \end{aligned}$$

TABLE 1: Numerical values of all the parameters used in U_{CKM_4} matrix [32–34].

CKM_4 Parameters	$m_{t'} = 400GeV$	$m_{t'} = 600GeV$
λ	0.227 ± 0.001	0.227 ± 0.001
A	0.801 ± 0.022	0.801 ± 0.002
C	0.38 ± 0.04	0.42 ± 0.04
$\delta_{ub'}$	1.24 ± 0.23	1.22 ± 0.24
p	1.45 ± 1.20	1.35 ± 1.53
q	0.16 ± 0.12	0.12 ± 0.07
r	0.30 ± 0.37	0.19 ± 0.27
$\delta_{ub'}$	1.21 ± 1.59	1.32 ± 1.76
$\delta_{cb'}$	1.10 ± 1.64	1.25 ± 1.81

$$\widetilde{V}_{cb} = A\lambda, \quad \widetilde{V}_{cb'} = q\lambda^2 e^{-\iota\delta_{cb'}}, \tag{11}$$

$$\widetilde{V}_{td} = A\lambda^3\left(1 - Ce^{\iota\delta_{ub}}\right) + r\lambda^4\left(qe^{-\iota\delta_{cb'}} - pe^{-\iota\delta_{ub'}}\right), \tag{12}$$

$$\widetilde{V}_{ts} = -A\lambda^2 - qr\lambda^3 e^{-\iota\delta_{cb'}} + \frac{A}{2}\lambda^4\left(1 + r^2 Ce^{\iota\delta_{ub}}\right),$$

$$\widetilde{V}_{tb} = 1 - \frac{r^2\lambda^2}{2}, \tag{13}$$

$$\widetilde{V}_{tb'} = r\lambda,$$

$$\widetilde{V}_{t'd} = \lambda^3\left(qe_{\iota\delta_{cb'}}\right) + Ar\lambda^4\left(1 + Ce^{\iota\delta_{ub}}\right), \tag{14}$$

$$\widetilde{V}_{t's} = q\lambda^2 e^{-\iota\delta_{ub'}} + Ar\lambda^3 + \lambda^4\left(-pe^{-\iota\delta_{ub'}} + \frac{q}{2}e_{\iota\delta_{cb'}} + \frac{qr^2}{2}e_{\iota\delta_{cb'}}\right), \tag{15}$$

$$\widetilde{V}_{t'b} = -r\lambda,$$

$$\widetilde{V}_{t'b} = 1 - \frac{r^2\lambda^2}{2}, \tag{16}$$

where all the elements of U_{CKM} are unitary up to $O(\lambda^4)$.

The above expansion corresponds to the Wolfenstein parametrization with $C = \sqrt{\rho^2 + \eta^2}$ and $\delta_{ub} = \tan^{-1}(\eta/\rho)$. Constraints on all the elements of CKM_4 matrix formulated using DK parametrization can be obtained by using the unitarity of the CKM_4 matrix. Through a variety of independent measurements, the SM 3×3 submatrix have been found to be approximately unitary. The values of CKM_4 parameters are taken from [32–34] where they perform the χ^2-fit at two values of t' mass i.e., $m_{t'} = 400GeV$ & $m_{t'} = 600GeV$. The 4th-generation quark masses are constrained to a narrow band, which increases the predictability of the SM_4. Along with that, they have also generated a fit for the 4 Wolfenstein parameters of the CKM matrix in the SM, in order to check for consistency with the standard fit. The results summarised are shown in Table 1. On the other hand, for the lepton mixing matrix U_{PMNS} for our analysis we have taken a basis where the charged lepton mass matrix is diagonal. Therefore, the lepton mixing matrix is simply $U_{PMNS} = U$. So, any complex symmetric 4×4 light neutrino mass matrix can be written as

$$M_\nu = UM_\nu^{\text{diag}}U^T, \tag{17}$$

where $M_\nu^{\text{diag}} = diag(m_1, m_2, m_3, m_4)$ is the diagonal form of the light neutrino mass matrix. The diagonalizing matrix U is the 4×4 version of the PMNS leptonic mixing matrix which is parametrized as [35]

TABLE 2: The upper limits obtained from NOνA, MINOS, Super-Kamiokande, IceCube and IceCube-DeepCore.

Experiment	$\theta_{24}^{PMNS_4}$	$\theta_{34}^{PMNS_4}$	$|U_{\mu4}|^2$	$|U_{\tau4}|^2$
NoνA	20.8	31.2	0.126	0.268
MINOS	7.3	26.6	0.016	0.20
SuperK	11.7	25.1	0.041	0.18
IceCube-DeepCore	19.4	22.8	0.11	0.15

TABLE 3: The limits obtained on sterile mixing angles.

Parameters	$\theta_{24}^{PMNS_4}$	$\theta_{34}^{PMNS_4}$
For $m_{t'} = 400GeV$	$6.57° - 23.36°$	$1.53° - 31.59°$
For $m_{t'} = 600GeV$	$6.87° - 23.15°$	$3.78° - 32.40°$
Parameters	$|U_{\mu4}|^2$	$|U_{\tau4}|^2$
For $m_{t'} = 400GeV$	$0.0003 - 0.0300$	$0.00 - 0.2031$
For $m_{t'} = 600GeV$	$0.0001 - 0.0236$	$0.00 - 0.1432$

TABLE 4: The upper limits of sterile mixing parameters obtained from model(QLC) and from NOνA, MINOS, Super-Kamiokande and IceCube-DeepCore.

Experiment	$\theta_{24}^{PMNS_4}$	$\theta_{34}^{PMNS_4}$	$|U_{\mu4}|^2$	$|U_{\tau4}|^2$
NoνA	20.8	31.2	0.126	0.268
MINOS	7.3	26.6	0.016	0.20
SuperK	11.7	25.1	0.041	0.18
IceCube-DeepCore	19.4	22.8	0.11	0.15
QLC Model	$\theta_{24}^{PMNS_4}$	$\theta_{34}^{PMNS_4}$	$|U_{\mu4}|^2$	$|U_{\tau4}|^2$
QLC(400 GeV)	23.36	31.59	0.030	0.203
QLC(600 GeV)	23.15	32.40	0.024	0.143

$$U = \widetilde{R}_{34}R_{24}\widetilde{R}_{14}R_{23}\widetilde{R}_{13}R_{12}, \tag{18}$$

where the rotation matrices R, $\widetilde{R}$ can be further parametrized as (for example R_{24} and $\widetilde{R}_{34}$)

$$R_{24} = \begin{bmatrix} 1 & 0 & 0 & 0 \\ 0 & 1 & 0 & 0 \\ 0 & C_{24} & 1 & S_{24} \\ 0 & -S_{24} & 0 & C_{24} \end{bmatrix}, \tag{19}$$

$$\widetilde{R}_{34} = \begin{bmatrix} 1 & 0 & 0 & 0 \\ 0 & 1 & 0 & 1 \\ 0 & 0 & C_{34} & S_{34}e^{\iota\phi} \\ 0 & 0 & -S_{34}e^{\iota\phi} & C_{34} \end{bmatrix}, \tag{20}$$

where $C_{ij} \equiv \cos\theta_{ij}$, $S_{ij} \equiv \sin\theta_{ij}$, and $\widetilde{S}_{ij} \equiv S_{ij}e^{-\iota\phi_{ij}}$ and here, ϕ_{ij} are the lepton Dirac CP phases. These phases are generalised as ϕ as these are unconstrained and we used the same range of spread for all $[0 - 2\pi]$ with flat distribution.

However, the values of the U_{PMNS_4} angles are taken as under at 1-σ level [38]

$$\sin^2\theta_{13} = 0.02206^{+0.00075}_{-0.00075}, \tag{21}$$

$$\sin^2\theta_{12} = 0.307^{+0.013}_{-0.012}, \tag{22}$$

$$\sin^2\theta_{23} = 0.538^{+0.033}_{-0.069}. \tag{23}$$

The value of CP violation phases ϕ have been kept open varying freely between $(0 - 2\pi)$ and the values used for θ_{14}, θ_{24} and θ_{34} are assumed to vary freely between $(0 - \pi/4)$. The reason behind this specific limit $(0 - \pi/4)$ is that all the values obtained using our reference experiments i.e. NoνA, MINOS, SuperK, and IceCube-DeepCore [39–43] vary between this similar range; so instead of taking a specific value, we have taken that whole range in our model. Table 2 shows all the upper limits obtained from various experiments.

After performing the Monte Carlo simulations we estimated the texture of the correlation matrix (V_{c_4}) for two different values of $m_{t'} = 400\,GeV\,\&\,600\,GeV$ (where $m_{t'}$ is the mass

$$U_{PMNS_4} = \begin{bmatrix} 0.5596\ldots0.5625 & 0.2235\ldots0.2314 & 0.1520\ldots0.1770 & 0.0131\ldots0.1975 \\ 0.3339\ldots0.3370 & 0.4181\ldots0.3370 & 0.4181\ldots0.4224 & 0.0180\ldots0.1732 \\ 0.0375\ldots0.1394 & 0.3310\ldots0.3485 & 0.4379\ldots0.4594 & 0.0076\ldots0.4507 \\ 0.0076\ldots0.01541 & 0.0062\ldots0.2154 & 0.0050\ldots0.2832 & 0.7332\ldots0.7596 \end{bmatrix}, \tag{24}$$

and the best fit obtained using a normal distribution of the observables including both quark and lepton parameters is in the form of the matrix below

$$U_{PMNS_4} = \begin{bmatrix} 0.5596\ldots0.5630 & 0.2259\ldots0.2337 & 0.1538\ldots0.1725 & 0.0140\ldots0.2240 \\ 0.5422\ldots0.5449 & 0.3304\ldots0.3325 & 0.4176\ldots0.4204 & 0.0130\ldots0.1538 \\ 0.07385\ldots0.1243 & 0.3345\ldots0.3450 & 0.4475\ldots0.4562 & 0.0070\ldots0.3784 \\ 0.0118\ldots0.1776 & 0.0042\ldots0.1919 & 0.0049\ldots0.2299 & 0.7438\ldots0.7565 \end{bmatrix}, \tag{26}$$

and the best fit obtained is

$$U_{PMNS_4} = \begin{bmatrix} 0.5619 & 0.2307 & 0.1631 & 0.1052 \\ 0.5437 & 0.3314 & 0.4190 & 0.0932 \\ 0.0994 & 0.3424 & 0.4548 & 0.1637 \\ 0.0783 & 0.1074 & 0.1044 & 0.7553 \end{bmatrix}. \tag{27}$$

As per our model procedure, in order to constrain the sterile neutrino parameters i.e., θ_{24}^{PMNS}, θ_{34}^{PMNS}, $|U_{\mu4}|^2$ and $|U_{\tau4}|^2$ we have used the inverse equation (8).

4.1. Predictions for θ_{24}^{PMNS} and θ_{34}^{PMNS}. We have investigated the implication of the nontrivial structure of the V_{c_4} correlation matrix in the light of the latest results of various experiments. After using the CKM_4 and $PMNS_4$ parametrization we obtain the structure of V_{c_4} from equation (2), the analytical equations used in order to calculate the values of sterile neutrino parameters analytically as well as numerically are as follows:

$$\theta_{24} = \cos\left(\theta_{14}\right)\sin\left(\theta_{24}\right)$$
$$\theta_{34} = e^{-\iota\phi}\cos\left(\theta_{14}\right)\cos\left(\theta_{24}\right)\sin\left(\theta_{34}\right)$$
$$|U_{\mu4}|^2 = \left(1 - \sin^2\left(\theta_{14}\right)\right)\sin^2\left(\theta_{24}\right) \tag{28}$$
$$|U_{\tau4}|^2 = \left(1 - \sin^2\left(\theta_{14}\right)\right)\left(1 - \sin^2\left(\theta_{24}\right)\right)\sin^2\left(\theta_{34}\right).$$

Tables 3 and 4 show the comparison of upper limits obtained above with the four different experimental results.

During the analysis of the above results, one can observe that values obtained by QLC(400/600 GeV) lie close to the results obtained from the NoνA and IceCube-DeepCore

of t') and implemented the same matrix in our inverse equation and obtained the constrained results for the sterile neutrino parameters. We obtained predictions for θ_{24} and θ_{34} and then compared our results with the current experimental bounds given by NoνA, MINOS, SuperK, and IceCube-DeepCore [39–43] experiments.

4. Results

We have divided our results into two parts i.e., for $m_{t'} = 400\,GeV$ and $m_{t'} = 600\,GV$. The $PMNS_4$ matrix obtained in case of $m_{t'} = 400\,GeV$ is

$$U_{PMNS_4} = \begin{bmatrix} 0.5614 & 0.2281 & 0.1642 & 0.1016 \\ 0.5450 & 0.3353 & 0.4203 & 0.0970 \\ 0.1006 & 0.3447 & 0.4557 & 0.1997 \\ 0.0775 & 0.1118 & 0.1406 & 0.7571 \end{bmatrix}. \tag{25}$$

In case of $m_{t'} = 600\,GeV\,PMNS_4$ is

experiments. Numerically in all four equations (23), the effect of the sterile neutrino mixing parameters can be clearly seen on one another. We report interrelated behaviour between $\sin^2\theta_{34}^{PMNS}$ and $\sin^2\theta_{24}^{PMNS}$ with the help of $3 - \sigma$ scattered plots in space of two sterile neutrino mixing angles θ_{34}^{PMNS} and θ_{24}^{PMNS} with the varying range of $\sin^2\theta_{12}^{PMNS}$ and $\sin^2\theta_{23}^{PMNS}$. The correlation between the solar and atmospheric mixing parameters $(\sin^2\theta_{12}^{PMNS}$ and $\sin^2\theta_{23}^{PMNS})$ and the active-sterile mixing parameter $(\sin^2\theta_{34}^{PMNS}$ and $\sin^2\theta_{24}^{PMNS})$ is shown in Figures 1–4.

Here, we note that the small mixing with sterile neutrinos will in general modify mixing scenarios. The mixing angles of active and sterile neutrinos are of order e/m_s, where e is any of the entries $\left(U_v^{4\times4}\right)_f$ with $f = e, \mu, \tau$ and m_s is the sterile neutrino mass. Deviations from initial mixing angles θ_{12}^{PMNS}, θ_{13}^{PMNS} and θ_{23}^{PMNS} are of the same order.

As our results vary upon the value $m_{t'} = 400\,GeV\,\&\,600\,GeV$ we have obtained histograms of the probability density function for θ_{24}^{PMNS} and θ_{34}^{PMNS} for both $400\,GeV\,\&\,600\,GeV$, respectively, and show comparison between the two. In Figures 5 and 6 we have shown this quite nicely the left panel of the figure is for $\theta_{24}^{PMNS}\,\&\,\theta_{34}^{PMNS}$ for $m_{t'} = 400\,GeV$, whereas the right panel shows the $\theta_{24}^{PMNS}\,\&\,\theta_{34}^{PMNS}$ for $m_{t'} = 600\,GeV$ respectively. We have analysed numerically the normal distributions of both the mixing angles through histograms in Figures 5 and 6. We have compared our results for the upper values from NoνA experiment. Here the dashed lines are for $\theta_{24}^{PMNS}\,\&\,\theta_{34}^{PMNS}$ (NoνA experiment), the thick solid lines are the 3-σ upper and lower values of θ_{24}^{PMNS} and θ_{34}^{PMNS} obtained using the QLC model.
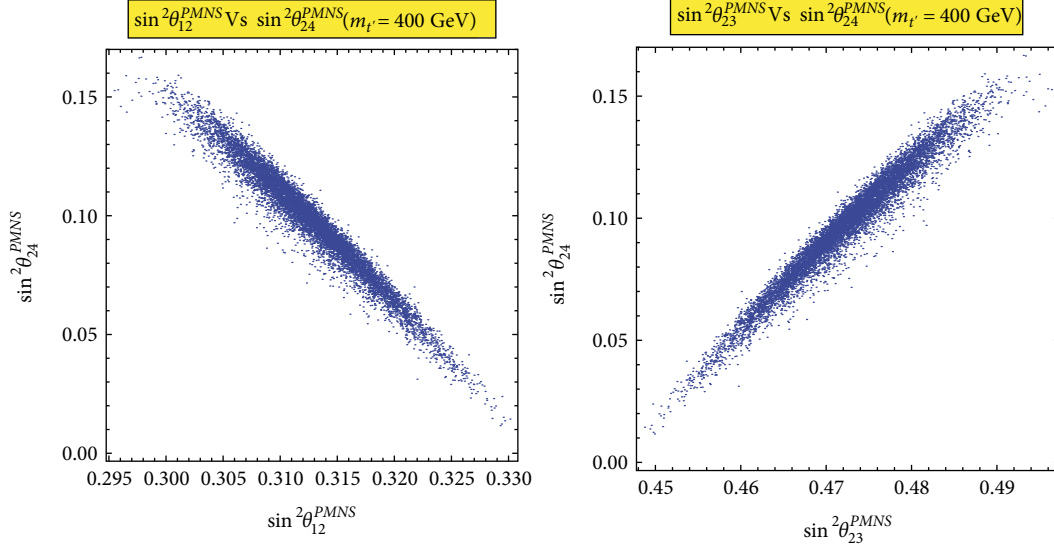
FIGURE 1: Correlation plot for $\sin^2 \theta_{24}^{PMNS}$ against $\sin^2 \theta_{12}^{PMNS}$ (left) and $\sin^2 \theta_{23}^{PMNS}$ (right) for $m_{t'} = 400 GeV$.
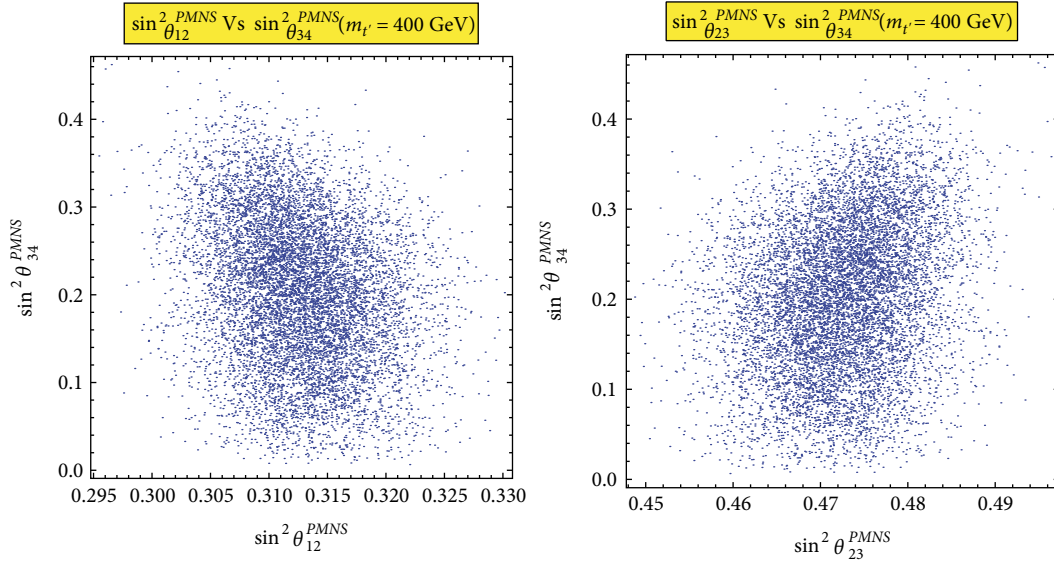

FIGURE 2: Correlation plot for $\sin^2 \theta_{34}^{PMNS}$ against $\sin^2 \theta_{12}^{PMNS}$ (left) and $\sin^2 \theta_{23}^{PMNS}$ (right) for $m_{t'} = 400 GeV$.

In order to analyse their impact more accurately, we have made contour plots in Figure 7. If, the mixing angles are expressed in terms of the relevant matrix elements (23), then the limits on θ_{34} and θ_{24} become $|U_{\mu 4}|^2$ and $|U_{\tau 4}|^2$ at the 99.7% C.L. i.e., 3σ range. This whole analysis is very less sensitive to θ_{14} which is constrained to be small by reactor experiments [44] as well as the QLC model analysis via which the value obtained is smaller as compared to the other two angles. The contour plots shown in the corresponding Figure 7 are depicting the correlation between θ_{34} and θ_{24} for $m_{t'} = 400 GeV$ & $600 GeV$ and $|U_{\mu 4}|^2$ and $|U_{\tau 4}|^2$ again for $m_{t'} = 400 GeV$ & $600 GeV$, respectively. These plots clearly depict constrained ranges of θ_{34} and θ_{24} as well as $|U_{\mu 4}|^2$ and $|U_{\tau 4}|^2$ which are comparable to the experimental results obtained by NoνA and IceCube-DeepCore [23, 24].

5. Conclusions

In the desire to understand the depth of the quark and lepton world and their varying scenario, the quark-lepton symmetry and unification field has drawn a lot of attention of many researchers in recent years. Out of the different aspects that imply the symmetry and unification in the quark and lepton sectors, the QLC relations between the mixing angles of the U_{CKM} and U_{PMNS} matrices have been considered very interesting and suggestive. Motivated by previous works towards its understanding, in this paper, we have made an attempt to take forward our previous work in a completely new direction to explain the QLC Model with sterile neutrinos. We have introduced a totally new approach of QLC involving the existence of sterile neutrino using 3 + 1 scenario.
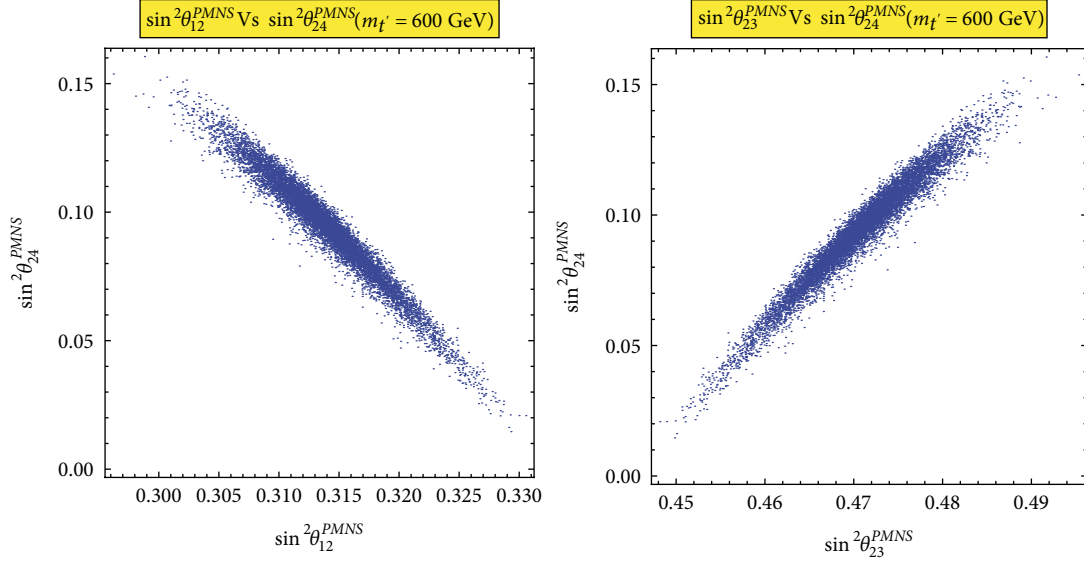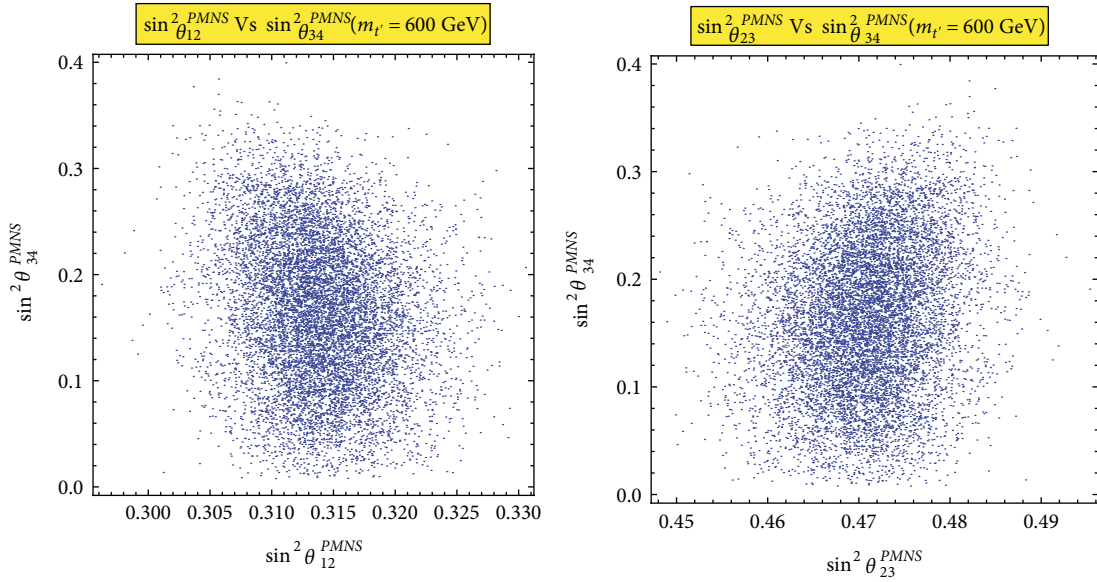
FIGURE 3: Correlation plot for $\sin^2 \theta_{34}^{PMNS}$ against $\sin^2 \theta_{12}^{PMNS}$ (left) and $\sin^2 \theta_{23}^{PMNS}$ (right) for $m_{t'} = 600 GeV$.

FIGURE 4: Correlation plot for $\sin^2 \theta_{34}^{PMNS}$ against $\sin^2 \theta_{12}^{PMNS}$ (left) and $\sin^2 \theta_{23}^{PMNS}$ (right) for $m_{t'} = 600 GeV$.

The detailed analysis is done for the non-trivial relation between the U_{PMNS_4} and U_{CKM_4} mixing matrices along with the phase mismatch between the quarks and leptons via ψ_4 the diagonal matrix phase. Using all the parameters that are available from the global data analysis we have investigated the structure of the correlation matrix V_{c_4} numerically for two different values of $m_{t'} = 400 GeV$ & $600 GeV$. We have obtained results for two sterile neutrino mixing angles i.e., θ_{24}^{PMNS} and θ_{34}^{PMNS} and two elements of the $PMNS_4$ mixing matrix i.e., $\left|U_{\mu 4}\right|^2$ and $\left|U_{\tau 4}\right|^2$ then compared the upper limits with different experiments mentioned above. We have compared just the upper limits because only the upper limits of all the parameters are available collectively in the recent results from these experiments [39–43]. The whole analysis gives us the hint about the relevance of the sterile neutrinos with the quark-lepton unification and the model we have been using i.e., Quark-Lepton Complementarity. The complete understanding of such a wide dissimilarity between the quark and lepton mixing patterns is considered to be one of the biggest challenges for the physics beyond the standard model.

In present world keeping in view all experiments these results are still favoured by the present experimental data within their measurement errors and if these QLC relations are not accidental, they strongly suggest the common connection between quarks and leptons at some high energy scale. Although, it is very hard to understand these type of relations
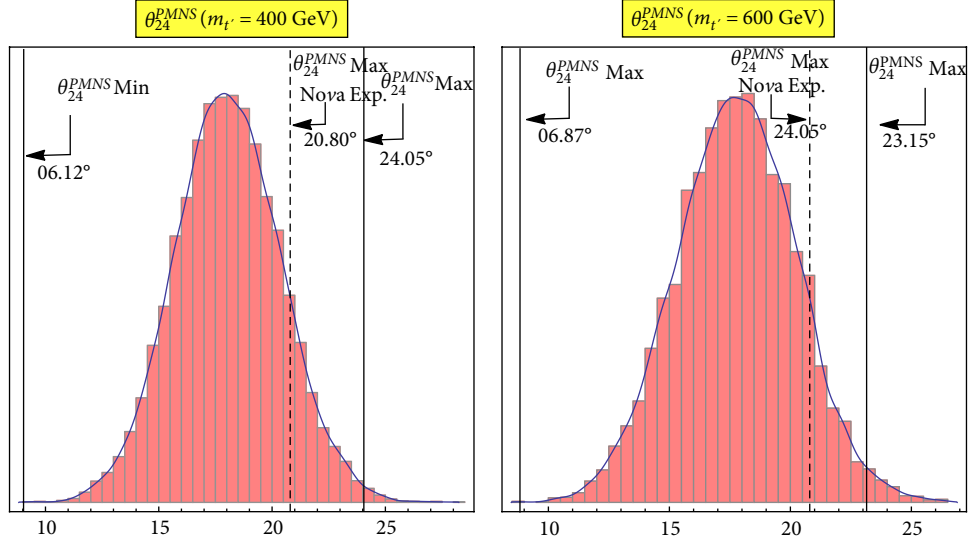
FIGURE 5: Probability density distribution of θ_{24}^{PMNS} for $m_{t'} = 400GeV$ (left) and $m_{t'} = 600GeV$ (right).
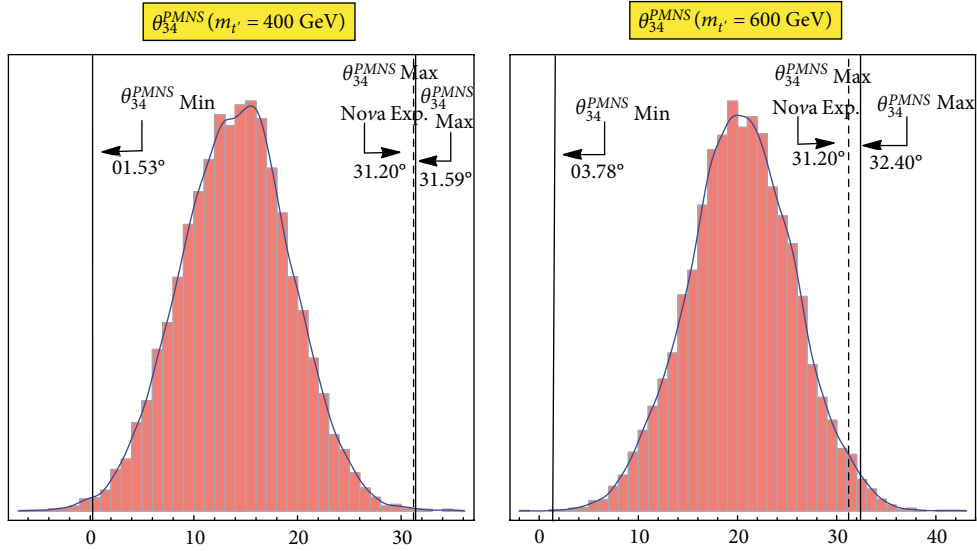

FIGURE 6: Probability density distribution of θ_{34}^{PMNS} for $m_{t'} = 400GeV$ (left) and $m_{t'} = 600GeV$ (right).
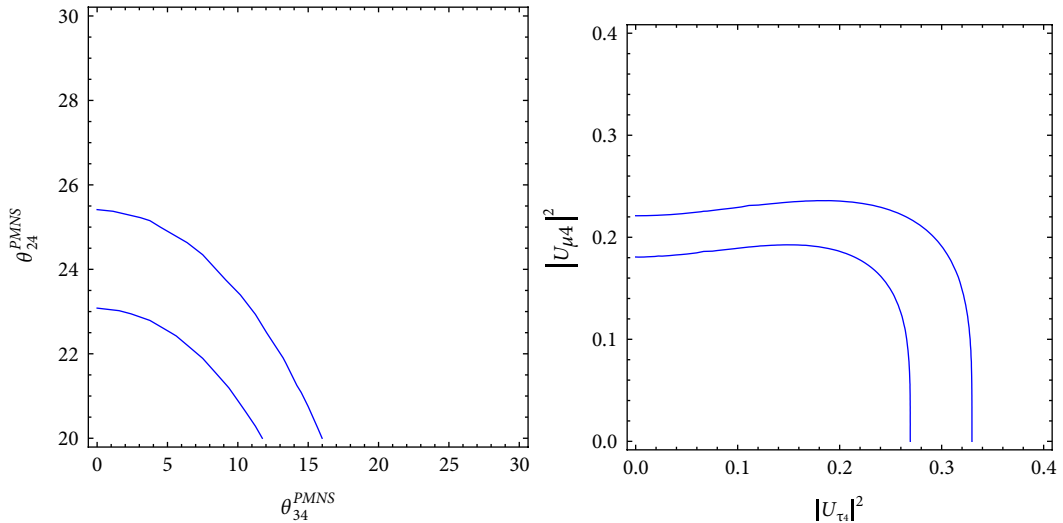

FIGURE 7: Contour plots between θ_{24}^{PMNS} and θ_{34}^{PMNS} (left) & $\left| U_{\mu 4} \right|^2$ and $\left| U_{\tau 4} \right|^2$ (right) where θ_{14}^{PMNS} is assumed to vary between $0 - \pi/4$.

in ordinary bottom-up approaches, where the quarks and leptons are treated separately with no specific connection seen between them. We do require some top-down approaches like the Grand Unified Theories(GUT) which sometimes also unify quarks and leptons and provide a framework to construct a model in which QLC relation can be embedded in a natural way. With this endeavor to perform numerical simulations in order to investigate the sterile neutrino mixing angles, one might have an eye to look forward towards the understanding of the QLC model in a better way. The connoisseur eye and deep knowledge with some theoretical ground can explain QLC relations precisely. The results obtained numerically and analytically in this paper can be noticed in a good agreement with the experimental data. As a concluding remark, we would like to add to above work that the way *sterile neutrinos* and *QL unification* have evolved with time, clearly indicates us about the possible significance of sterile neutrinos with QLC and also that there could be the possibility of existence of sterile neutrinos when $\theta_{23} < \pi/4$ (atmospheric angle lies in 1st octant). We look forward to the experimental verification of these predictions.

Data Availability

The numerical data used to support the findings of this study are included within the article along with proper citations.

Conflicts of Interest

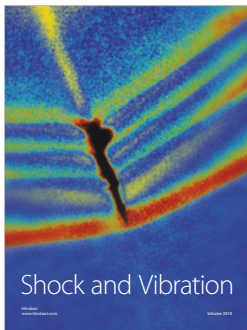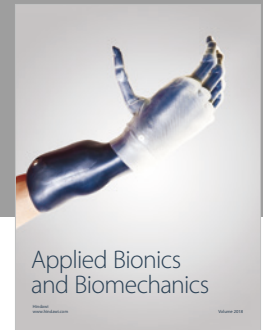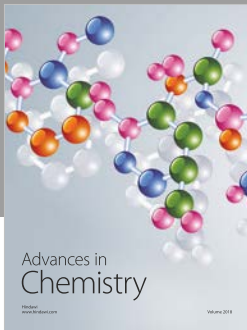The authors declare that they have no conflicts of interest.

Acknowledgments

References

[1] F. An, J. Z. Bai, A. B. Balantekin et al., "Observation of electron-antineutrino disappearance at daya bay," *Physical Review Letters*, vol. 108, Article ID 171803, 2012.

[2] J. Ahn, "Observation of reactor electron antineutrinos disappearance in the RENO experiment," *Physical Review Letters*, vol. 108, Article ID 191802, 2012.

[3] K. Abe, "Indication of electron Neutrino appearance from an accelerator-produced off-axis muon neutrino beam," *Physical Review Letters*, vol. 107, Article ID 041801, 2011.

[4] P. Adamson, "Improved search for muon-neutrino to electron-neutrino oscillations in MINOS," *Physical Review Letters*, vol. 107, Article ID 181802, 2011.

[5] Y. Abe, "Reactor ve disappearance in the double chooz experiment," *Physical Review D*, vol. 86, Article ID 052008, 2012.

[6] G. L. Fogli, E. Lisi, A. Marrone, D. Montanino, A. Palazzo, and A. M. Rotunno, "Global analysis of neutrino masses, mixings, and phases: Entering the era of leptonic CP violation searches," *Physical Review D*, vol. 86, no. 1, p. 013012, 2012.

[7] M. C. Gonzalez-Garcia, M. Maltoni, J. Salvado, and T. Schwetz, "Global fit to three neutrino mixing: critical look at present precision," *Journal of High Energy Physics*, vol. 2012, no. 12, p. 123, 2012.

[8] D. Forero, M. Tortola, and J. Valle, "Global status of neutrino oscillation parameters after neutrino-2012," *Physics Review D*, vol. 86, no. 7, Article ID 073012, 2012.

[9] H. Georgi and C. Jarlskog, "A new lepton - quark mass relation in a unified theory," *Physics Letters B*, vol. 86, no. 3–4, pp. 297–300, 1979.

[10] H. Minakata and A. Y. Smirnov, "Neutrino mixing and quark-lepton complementarity," *Physical Review D*, vol. 70, no. 7, Article ID 073009, 2004.

[11] W. Rodejohann, "A parameterization for the neutrino mixing matrix," *Physical Review D*, vol. 69, no. 3, Article ID 033005, 2004.

[12] K. A. Hochmuth and W. Rodejohann, "Low and high energy phenomenology of quark-lepton complementarity scenarios," *Physical Review D*, vol. 75, no. 7, Article ID 073001, 2007.

[13] S. K. Agarwalla, M. K. Parida, R. N. Mohapatra, and G. Rajasekaran, "Neutrino mixings and leptonic CP violation from CKM matrix and majorana phases," *Physical Review D*, vol. 75, no. 3, Article ID 033007, 2007.

[14] G. Abbas, S. Gupta, G. Rajasekaran, and R. Srivastava, "High scale mixing unification for dirac neutrinos," *Physical Review D*, vol. 91, no. 11, Article ID 111301, 2015.

[15] J. Ferrandis and S. Pakvasa, "A prediction for |U(e3)| from patterns in the charged lepton spectra," *Physical Letter B*, vol. 603, p. 184, 2004.

[16] P. H. Frampton and R. N. Mohapatra, "Possible gauge theoretic origin for quark-lepton complementarity," *Journal of High Energy Physics*, vol. 2005, no. 1, p. 025, 2005.

[17] S. Antusch, S. F. King, and R. N. Mohapatra, "Quark-lepton complementarity in unified theories," *Physical Letters B*, vol. 618, no. 1–4, pp. 150–161, 2005.

[18] E. Ma, "Triplicity of quarks and leptons," *Modern Physics Letters A*, vol. 20, no. 26, pp. 1953–1959, 2005.

[19] M. Picariello, B. C. Chauhan, J. Pulido, and E. Torrente-Lujan, "Predictions from non trivial quark-lepton complementarity," *International journal of Modern Physics A*, vol. 22, no. 31, pp. 5860–5874, 2008.

[20] B. C. Chauhan, M. Picariello, J. Pulido, and E. Torrente, "Quark–lepton complementarity with lepton and quark mixing data predict $\theta_{13}^{PMNS}=(9^{+1}_{-2})^{\circ}$," *European Physics Journal C*, vol. 50, pp. 573–578, 2007.

[21] G. Sharma and B. C. Chauhan, "Quark-lepton complementarity predictions for θ_{23}^{PMNS} and CP violation," *Journal of High Energy Physics*, vol. 2016, no. 7, 2016.

[22] G. Sharma, S. Bhardwaj, B. C. Chauhan, and S. Verma, "Quark-lepton complementarity model-based predictions for θ_{23}^{PMNS} with neutrino mass hierarchy," *Springer Proceedings in Physics*, vol. 203, pp. 251–256, 2018.

[23] M. A. Acero, P. Adamson, L. A. T. Alion et al., "New constraints on oscillation parameters from νe appearance and νμ disappearance in the NOvA experiment," *Physical Review D*, vol. 98, p. 032012, 2018.

[24] D. Williams, "Recent results from icecube," *International Journal of Modern Physics: Conference Series*, vol. 46, Article ID 1860048, 2018.

[25] A. Djouadi and A. Lenz, "Sealing the fate of a 4th generation of fermions," *Physics Letters B*, vol. 715, no. 4-5, pp. 310–314, 2012.

[26] E. Kuflik , Y. Nir, and T. Volansky, "Implications of higgs searches on the four generation standard model," *Physical Review Letters*, vol. 110, no. 9, Article ID 091801, 2013.

[27] S. Bar-Shalom, S. Nandi, and A. Soni, "Two higgs doublets with 4th generation fermions - models for TeV-scale compositeness," *Physical Review D*, vol. 84, no. 5, Article ID 053009, 2011.

[28] S. Bar-Shalom, M. Geller, S. Nandi, and A. Soni, "Two higgs doublets, a 4th generation and a 125 GeV Higgs: a review," *Advances High Energy Physics*, vol. 2013, Article ID 672972, pp. 1–28, 2013.

[29] X.-G. He and G. Valencia, "An extended scalar sector to address the tension between a 4th generation and Higgs searches at the LHC," *Physical Letters B*, vol. 707, no. 3–4, pp. 381–384, 2012.

[30] S. Chamorro-Solano , A. Moyotl , and M. A. Perez , "Lepton flavor changing Higgs Boson decays in a two higgs doublet model with a 4th generation of fermions," *Journal of Physics G: Nuclear and Particle Physics*, vol. 45, Article ID 7075003, 2018, https://arxiv.org/abs/1707.00100.

[31] D. Das, A. Kundu, and I. Saha, "Higgs data does not rule out a sequential 4th generation with an extended scalar sector," *Physical Review D*, vol. 97, no. 1, Article ID 011701, 2018.

[32] C. S. Kim and A. S. Dighe, " Tree FCNC and non-unitarity of CKM matrix," *International Journal of Modern Physics E*, vol. 16, no. 5, pp. 1445–1461, 2007.

[33] A. K. Alok, A. Dighe, and S. Ray, "CP asymmetry in the decays B→(Xs, Xd)mu+mu− with four generations," *Physical Review D*, vol. 79, no. 3, p. 034017, 2009.

[34] A. K. Alok, A. Dighe, and D. London, "Constraints on the Four-Generation Quark Mixing Matrix from a Fit to Flavor-Physics Data," *Physical Review D*, vol. 83, no. 7, Article ID 073008, 2011.

[35] N. Klop and A. Palazzo , "Imprints of CP violation induced by sterile neutrinos in T2K data," *Physical Review D*, vol. 91, no. 7, Article ID 073017, 2015.

[36] J. Schechter and J. W. F. Valle, "Neutrino masses in SU(2)×U(1) theories," *Physical Review D*, vol. 22, no. 9, pp. 2227–2235, 1980.

[37] B. Barry , W. Rodejohann, and H. Zhang, "Light sterile neutrinos: models and phenomenology," *Journal of High Energy Physics*, vol. 2011, no. 7, 2011.

[38] I. Esteban, M. C. Gonzalez-Garcia, M. Maltoni, I. Martinez-Soler, and T. Schwetz, "Updated fit to three neutrino mixing: exploring the accelerator-reactor complementarity," *Journal of High Energy Physics*, vol. 2017, no. 1, pp. 16–45, 2017.

[39] P. Adamson, L. Aliaga, D. Ambrose et al., "Search for active-sterile neutrino mixing using neutral-current interactions in NovA," *Physical Review D*, vol. 96, no. 7, 2017.

[40] Erica Smith, "Results from the NovA experiment," *International Journal of Modern Physics Conference Series*, vol. 46, Article ID 18600388, 2018.

[41] P. Adamson, I. Anghel, A. Aurisano et al., "Search for sterile neutrinos mixing with muon neutrinos in MINOS," *Physical Review Letters*, vol. 117, Article ID 151803, 2016.

[42] K. Abe, Y. Haga, Y. Hayato et al., "Limits on sterile neutrino mixing using atmospheric neutrinos in Super-Kamiokande," *Physical Review D*, vol. 91, Article ID 52019, 2015.

[43] M. G. Aartsen, M. Ackermann, J. Adams et al., "Search for sterile neutrino mixing using three years of icecube deepcore data," *Physical Review D*, vol. 95, no. 11, Article ID 112002, 2017.

[44] G. Mention, M. Fechner, T. Lasserre et al., "The reactor antineutrino anomaly," *Physical Review D*, vol. 83, no. 7, Article ID 073006, 2011.